



PAPER

Development of a novel fibre optic beam profile and dose monitor for very high energy electron radiotherapy at ultrahigh dose rates

OPEN ACCESS

RECEIVED

4 December 2023

REVISED

5 March 2024

ACCEPTED FOR PUBLICATION

13 March 2024

PUBLISHED

3 April 2024

Original content from this work may be used under the terms of the [Creative Commons Attribution 4.0 licence](#).

Any further distribution of this work must maintain attribution to the author(s) and the title of the work, journal citation and DOI.



Joseph J Bateman¹ , Emma Buchanan², Roberto Corsini², Wilfrid Farabolini², Pierre Korysko^{1,2}, Robert Garbrecht Larsen^{2,3} , Alexander Malyzhenkov², Iñaki Ortega Ruiz², Vilde Rieker^{2,4}, Alexander Gerbershagen³ and Manjit Dosanjh^{1,2}

¹ John Adams Institute for Accelerator Science, Department of Physics, University of Oxford, Oxford, OX1 3RH, United Kingdom

² European Organization for Nuclear Research (CERN), Meyrin, 1211, Geneva, Switzerland

³ Particle Therapy Research Centre (PARTREC), Department of Radiation Oncology, University Medical Centre Groningen, University of Groningen, Groningen, The Netherlands

⁴ Department of Physics, University of Oslo, NO-0316 Blindern, Oslo, Norway

E-mail: Manjit.Dosanjh@cern.ch

Keywords: FLASH, cherenkov, VHEE, fibre dosimetry

Supplementary material for this article is available [online](#)

Abstract

Objective. Very high energy electrons (VHEE) in the range of 50–250 MeV are of interest for treating deep-seated tumours with FLASH radiotherapy (RT). This approach offers favourable dose distributions and the ability to deliver ultra-high dose rates (UHDR) efficiently. To make VHEE-based FLASH treatment clinically viable, a novel beam monitoring technology is explored as an alternative to transmission ionisation monitor chambers, which have non-linear responses at UHDR. This study introduces the fibre optic flash monitor (FOFM), which consists of an array of silica optical fibre-based Cherenkov sensors with a photodetector for signal readout. *Approach.* Experiments were conducted at the CLEAR facility at CERN using 200 MeV and 160 MeV electrons to assess the FOFM's response linearity to UHDR (characterised with radiochromic films) required for FLASH radiotherapy. Beam profile measurements made on the FOFM were compared to those using radiochromic film and scintillating yttrium aluminium garnet (YAG) screens. *Main results.* A range of photodetectors were evaluated, with a complementary-metal-oxide-semiconductor (CMOS) camera being the most suitable choice for this monitor. The FOFM demonstrated excellent response linearity from 0.9 Gy/pulse to 57.4 Gy/pulse ($R^2 = 0.999$). Furthermore, it did not exhibit any significant dependence on the energy between 160 MeV and 200 MeV nor the instantaneous dose rate. Gaussian fits applied to vertical beam profile measurements indicated that the FOFM could accurately provide pulse-by-pulse beam size measurements, agreeing within the error range of radiochromic film and YAG screen measurements, respectively. *Significance.* The FOFM proves to be a promising solution for real-time beam profile and dose monitoring for UHDR VHEE beams, with a linear response in the UHDR regime. Additionally it can perform pulse-by-pulse beam size measurements, a feature currently lacking in transmission ionisation monitor chambers, which may become crucial for implementing FLASH radiotherapy and its associated quality assurance requirements.

1. Introduction

Treatment of deep-seated tumours (>5 cm) with electrons is expected to become possible in the coming years with the use of very high energy electron (VHEE) beams. Electrons with energies in the range 50–250 MeV could be used as a new radiotherapy modality due to recent advances in accelerator technology such as the high-gradient x-band radiofrequency (RF) electron acceleration cavities—developed as part of the CLIC study at CERN (Zha and Grudiev 2017)—as well as novel compact C-band RF systems (Faillace *et al* 2022). Therefore it

is possible to attain the higher energies required for electrons to reach deep-seated tumours with machines that could feasibly be located in a hospital campus. The main advantages of this modality are the increased penetration to depths >20 cm into the body and the sharper lateral penumbra in comparison to current clinical electron beams (DesRosiers *et al* 2000). In addition, the reduced scattering within the inhomogeneous tissues in the patient, due to the high relativistic inertia of the electrons at these energies (Lagzda *et al* 2020), allows the possibility to treat deep-seated tumours through the use of pencil beam scanning (PBS) (Bazalova-Carter *et al* 2015, Schuler *et al* 2017, Muscato *et al* 2023) and focussing (Kokurewicz *et al* 2019, Kokurewicz *et al* 2021, Whitmore *et al* 2021). Furthermore these intensity-modulated treatments have the potential for greater precision and conformity than is possible with photons. The higher beam intensities achievable with the proposed technology for VHEE, makes it an attractive choice for the delivery of ultrahigh dose rate (UHDR) radiotherapy. In fact it is technologically easier to generate high intensity electron beams in comparison to both UHDR MV photons and UHDR protons utilising the Bragg peak. For photons the bremsstrahlung production rate for x-ray targets is a limiting factor (Montay-Gruel *et al* 2022), while for protons the degraders required to generate a spread-out Bragg peak reduce the beam intensity (Jolly *et al* 2020). The use of VHEE beams allows a higher dose to be delivered over larger areas of tumorous tissue regions and hence is a promising candidate for potentially being able to elicit the FLASH effect in deep-seated tumours (Böhlen *et al* 2021).

The FLASH effect is a fairly recently discovered phenomenon observed in numerous *in vivo* radiobiological and animal studies which have demonstrated that delivering the prescribed dose of radiation at UHDR causes less damage to healthy tissue than when it is delivered at conventional dose rates, while still maintaining the same tumour control efficacy (Favaudon *et al* 2014, Loo *et al* 2017, Montay-Gruel *et al* 2017, Montay-Gruel *et al* 2019, Vozenin *et al* 2019). Determining the dose delivery parameters at which the FLASH effect is observable is still a huge area of research. Current preclinical data seem to suggest that delivering doses in excess of 10 Gy within a total delivery time of <500 ms, at a mean dose rates of >40 Gy s⁻¹, are reasonable values to observe a significant FLASH effect (Wilson *et al* 2020, Montay-Gruel *et al* 2021, Rothwell *et al* 2021, Vozenin *et al* 2022). While the delivery of VHEE at UHDR to elicit the FLASH effect offers a promising new paradigm in radiotherapy, many challenges still need to be overcome to consider this modality feasible for translation at the clinical level.

Perhaps one of the most important technological challenges for the clinical translation of FLASH radiotherapy is related to the difficulty of real-time dosimetry and beam monitoring at UHDR. This has been extensively reported in the literature (Romano *et al* 2022), and is largely due to the fact that for UHDR beams—more specifically ultrahigh dose-per-pulse beams—ionisation chambers exhibit large non-linearities in the form of recombination effects caused by the high charge density in each pulse of radiation (Pettersson *et al* 2017). This effect is much more prominent for modalities where the delivery of the radiation is from a pulsed linear accelerator, for example VHEE, since the instantaneous dose rate within each pulse is extremely high to obtain the required mean dose rates. The presence of this effect has already been demonstrated with VHEE and characterised with two separate ionisation chambers, namely the PTW Advanced Markus Chamber (McManus *et al* 2020) and the PTW Roos Chamber (Poppinga *et al* 2020).

Extensive work has been done to calculate corrections for the non-linearities in the response of ionisation chambers at UHDR, however these correction factors introduce large uncertainties into the dose measurements in the UHDR regime. Furthermore, the research into correcting the response of ionisation chambers at UHDR has primarily been focussed on parallel plate ionisation chambers for secondary standard dosimetry, as opposed to large area transmission ionisation chambers, used for beam monitoring, for which only limited studies have been conducted (Konradsson *et al* 2020).

Therefore, alternative dosimetry technologies need to be investigated for such modalities. The ideal characteristics for online beam monitoring technologies to be used for UHDR RT are (Romano *et al* 2022):

- a large dynamic intensity range in order to deal with beam intensities from conventional RT dose rates up to UHDR regime;
- a high temporal resolution in order to resolve pulses to determine instantaneous dose rate as well as provide feedback signal for accelerator's safety interlock;
- a high spatial resolution to provide beam position and profile measurements;
- a large sensitive area to be able to monitor the beam over the maximal extent of the clinical treatment fields, that can vary from less than one centimetre up to tens of centimetres;
- a high radiation tolerance since these detectors are a permanent fixture in the machine;
- a high level of beam transparency in order to minimise perturbations to the beam characteristics.

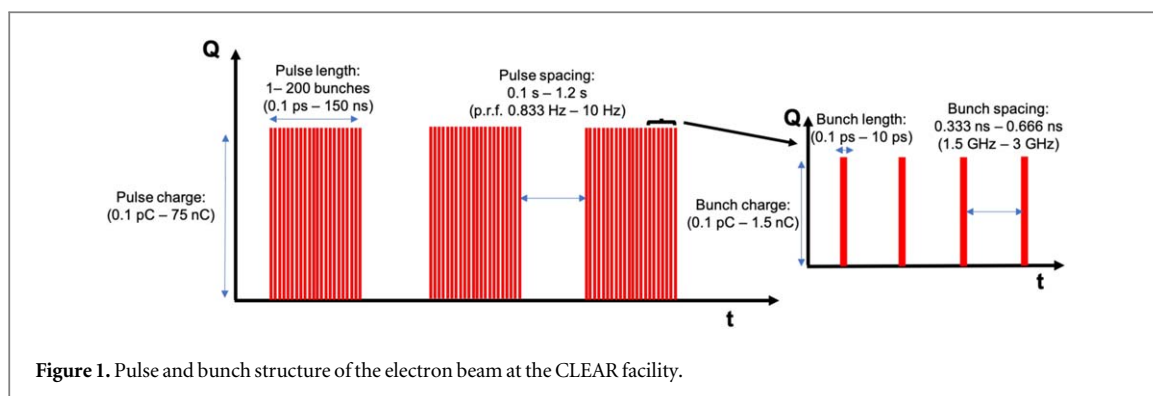


Figure 1. Pulse and bunch structure of the electron beam at the CLEAR facility.

While the majority of the research into UHDR real-time dosimetry has been focussed on detectors for reference dosimetry, a number of research groups have been investigating novel methods for UHDR beam monitoring, including the use of integrated current transformers (ICTs) (Oesterle *et al* 2021), air fluorescence (Trigilio *et al* 2022), SiC detectors (Romano *et al* 2023), and a scintillating screen named the 'FLASH Beam Scintillator Monitor' (FBSM) (Levin *et al* 2023).

The use of optical fibre-based methods, i.e. scintillator-coupled optical fibres and fibre optic Cherenkov sensors, for real-time dosimetry at UHDR has been of particular interest for its favourable properties such as dose-rate linearity and high spatial and temporal resolution, with numerous works demonstrating its applicability to real-time dosimetry and pulse monitoring for UHDR beams with electrons (Favaudon *et al* 2019, Jeong *et al* 2021, Ashraf *et al* 2022, Vanreusel *et al* 2022), protons (Kanouta *et al* 2023), and kVp x-rays (Hart *et al* 2022). A technique utilising scintillating fibres has been implemented on the secondary beamlines in the experimental areas at CERN for beam intensity and profile monitoring. The detector consists of an array of scintillating plastic fibres that are read-out using multi-channel silicon photomultipliers (SiPMs) (Ortega Ruiz *et al* 2020). Similar devices have also been developed in recent years for beam fluence and profile monitoring for hadron therapy centres (Leverington *et al* 2018, Allegrini *et al* 2021), however these devices have only been tested and optimised for PBS dose rates. In radiation therapy scintillation fibre dosimetry, Cherenkov radiation is often considered a source of contamination to the scintillation signal. However, direct detection of Cherenkov signal using optical fibres could be particularly beneficial within UHDR dosimetry since the increased beam intensity associated with this modality favours the detection of the optical photons produced in Cherenkov radiation (Ashraf *et al* 2020). Furthermore, Cherenkov light is produced instantaneously, on a timescale of 10^{-12} s, following the interaction between the charged particle and the dielectric medium, hence making it an ideal method for radiation detection at the fast time scales required for UHDR RT. Since the electrons in VHEE beams are relativistic, the relative variation of the angle of emission of Cherenkov radiation is minimal within the VHEE energy range (0.12% difference between 50 and 250 MeV) and therefore a Cherenkov based detector could be more suitable for VHEE dosimetry. A novel detector consisting of an array of optical fibre-based Cherenkov sensors connected to a photodetector is proposed as an alternative technology for UHDR online monitoring of the beam profile and dose, particularly for use with VHEE beams. In this work the development of such a detector, called the fibre optic flash monitor (FOFM) is outlined along with the initial characterisations of the first array prototype with 160 MeV and 200 MeV electron pencil beams at the CLEAR facility.

2. Materials and methods

2.1. CLEAR facility

The CERN Linear Electron Accelerator for Research (CLEAR) is a user facility at CERN that is independent from the main accelerator complex. It produces electron pulses with energies between 60 and 220 MeV and values of the charge-per-pulse ranging from 10 pC to a maximum achievable value of approximately 75 nC. The charge is measured using ICTs at different positions along the linear accelerator. The pulses (also called trains) are delivered at a repetition frequency (p.r.f.) that can be varied between 0.833 Hz (nominal) and 10 Hz and have a width with values in the range, approximately, from 0.1 ps (single bunch) to 150 ns (Sjebak *et al* 2019). Each train is sub-divided in shorter bunches, of order of picoseconds duration, spaced at a frequency of either 1.5 GHz or 3 GHz. The pulse structure of the CLEAR electron beam is shown in figure 1. The main focus of the CLEAR facility operation is on general accelerator R&D and component studies for existing and possible future accelerator applications. This includes studies of methods for high-gradient acceleration and prototyping and validation of accelerator components for beam diagnostics. The facility is also used to study radiation damage to electronics and for irradiations for medical applications. Indeed research in medical applications at CLEAR has

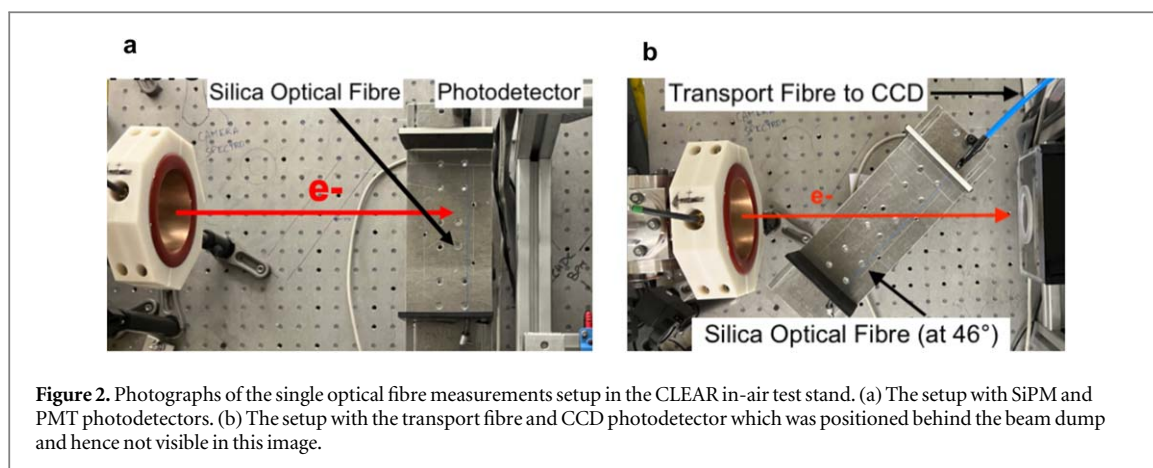


Figure 2. Photographs of the single optical fibre measurements setup in the CLEAR in-air test stand. (a) The setup with SiPM and PMT photodetectors. (b) The setup with the transport fibre and CCD photodetector which was positioned behind the beam dump and hence not visible in this image.

gained significant interest in recent years thanks to the facility's unique capability to deliver electron beams whose parameters (energy and intensity) are in the range required to study the feasibility of VHEE and UHDR RT (Korysko *et al* 2023a). At present numerous studies have been conducted, and many are still ongoing, to research the possible mechanisms behind the FLASH effect; as well as to test the feasibility of novel technologies for the delivery, characterisation, dosimetry and monitoring of these unconventional beams. The results of some of the experiments on the latter are described in this work.

2.2. Silica optical fibre monitor

2.2.1. Silica optical fibres

The FOFM beam dose and profile monitor consists of two main components, the fibre optic radiation sensors (FORS) where the Cherenkov signal is produced upon the delivery of the radiation and a photodetector to measure the optical Cherenkov photons transported within the silica optical fibre. The initial tests conducted as part of the development of the FOFM, were carried out using only a single fibre, specifically a 200 μm core diameter, 0.5 numerical aperture, step index multimodal silica optical fibre (Thorlabs GmbH, Munich, Germany), 20 cm long, coupled to photodetectors either directly (figure 2(a)) or through a 1.2 m long transport fibre (figure 2(b)).

Subsequent measurements involved an array of 28 fused silica optical fibres, 0.4 mm in diameter and 30 cm in length (Hilgenberg GmbH, Malsfeld, Germany) and the layout of the setup is shown in figure 3.

2.2.2. Photodetectors

Various photodetectors were tested in different configurations.

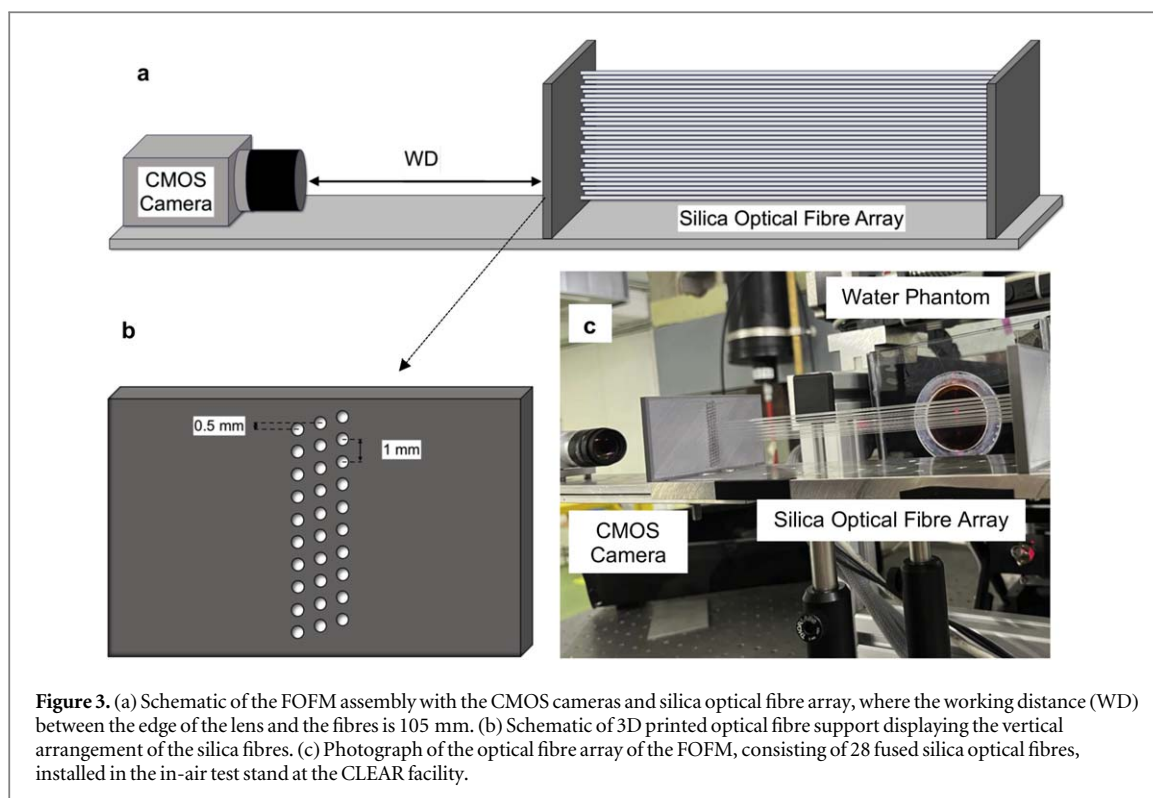
Specifically, the sensitive region of the single silica optical fibre was coupled:

- directly to a SiPM (Hamamatsu Photonics, Shizouka, Japan) in turn connected to a digitiser;
- directly to a fast photomultiplier tube (PMT) with a neutral density (ND) = 6.0 optical filter ($1 \times 10^{-4}\%$ transmission) (Thorlabs GmbH, Munich, Germany);
- to a charge coupled device (CCD) 6 MP camera (Retiga R6, Teledyne Photometrics, Thousand Oaks, US) housed within a black box, through a 1.2 m long transport fibre. In this case the sensitive region was positioned at 46° with respect to the direction of the electron beam. The CCD camera was operated at 14-bit pixel depth which has a 7 frames s^{-1} acquisition rate, with an exposure time of 1200 ms.

For the FOFM fused silica optical fibre array, a 2.3 MP Basler ace complementary-metal-oxide-semiconductor (CMOS) camera (Basler AG, Ahrensburg, Germany), with a Fujinon H525HA-1B 1:1.4/25 mm lens (Fujifilm Corporation, Tokyo, Japan) was used as photodetector. The CMOS camera was operated at 8-bit pixel depth at an acquisition rate of 42 frames s^{-1} and 0.034 ms exposure time. Before any data analysis was performed, background subtraction and noise removal were applied to the raw recorded data.

2.3. Radiochromic film dosimetry

Gafchromic EBT3, EBT-XD, MD-V3 and HD-V2 films (Ashland Inc., Bridgewater, NJ, USA) were used for radiochromic film dosimetry since they are well suited for the UHDR regime (Jaccard *et al* 2017). Specifically, for the measurements involving the response of the single optical fibre, dose-to-water calibrations were carried out



by irradiating Gafchromic EBT3 and MD-V3 films to the same beam conditions as the optical fibre. Direct dose-to-water calibrations for the response of the FOFM optical fibre array were performed using EBT-XD films, while the FOFM beam profile measurement comparisons in air were conducted using HD-V2 and MD-V3 films.

Each of the radiochromic films was scanned using an Epson Perfection V800 Photo scanner (Epson, Long Beach, US) at least 24 h after irradiation. Dose-to-water calibrations for all of the film types were obtained with a 5.5 MeV electron beam at a dose rate of 0.05 Gy s^{-1} , at a depth of 10 mm in solid water phantom with an SSD of 100 cm on the Oriatron eRT6 at CHUV Hospital, Lausanne, Switzerland (Jaccard *et al* 2018). For each point on the calibration curve the dose was measured using a PTW Advanced Markus Ionisation Chamber (PTW, Freiburg, Germany).

A custom Python script was used for the calibration and analysis of radiochromic films, which followed the single channel procedure defined in Micke *et al* (2011). Calibrations were performed with low energy electron beams since no standardised procedure currently exists for VHEE beams. The reported agreement between radiochromic film measurements and Monte Carlo simulations made with 165 MeV electrons for radiochromic films calibrated to clinical 20 MeV electron beams (Subiel *et al* 2014), as well as for 156 MeV electron beams at CLEAR calibrated to clinical 15 MeV electron beams (Lagzda *et al* 2020, Böhlen *et al* 2021), demonstrates the feasibility of using radiochromic films calibrated using low energy electron beams until it is possible to carry out this procedure with VHEE beams.

It must be pointed out however that, in other modalities, energy dependence (notably for kVp x-rays) (Chan *et al* 2023, Guan *et al* 2023a) and LET dependence (seen in protons) (Guan *et al* 2023b) in radiochromic films have been observed. A dose rate dependency has also been reported when using UHDR protons (Villoing *et al* 2022). Studies are currently ongoing at the CLEAR facility to validate and confirm any dose rate and energy dependence, using various passive dosimeters such as alanine and TLDS.

To obtain the dose-to-water calibrations for the single fibre response, the radiochromic film was positioned at a depth of 150 mm in a water phantom using the CLEAR C-robot (Korysko *et al* 2023b). During the film analysis a 2D Gaussian fit was applied to the dose distribution on the film and the dose was obtained by averaging the values within a circle of radius 5 mm centred on the mean of the Gaussian fit for the green channel. For the FOFM optical fibre array profile comparison, the projection of the y -axis profile is plotted, and a 1D Gaussian fit is applied whereby the standard deviation of this Gaussian fit is obtained and compared to the standard deviation of the Gaussian fit applied to the FOFM beam profile measurements.

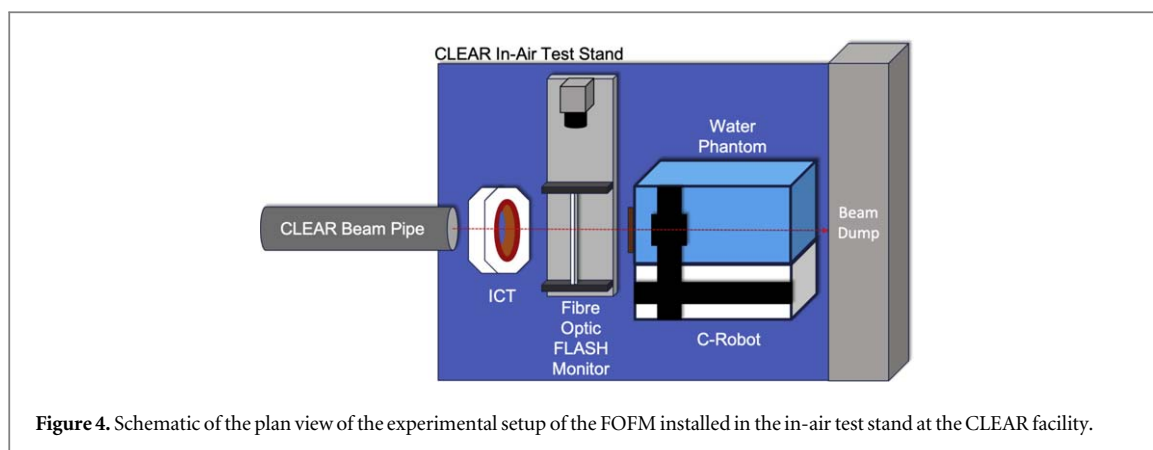


Figure 4. Schematic of the plan view of the experimental setup of the FOFM installed in the in-air test stand at the CLEAR facility.

2.4. Experimental setup

The single-fibre and 28-fibres array sensors were installed on the in-air test stand at the CLEAR facility, according to the schematic layout shown in figure 4 (with the exception of the single fibre case and CCD camera as photodetector, where the sensitive region of the optical fibre was oriented at 46° and had a transport fibre leading to the CCD). The ICT is used to measure the charge of each electron pulse. The C-Robot (Korysko *et al* 2023b) is used to pick up both radiochromic films and the scintillating yttrium aluminium garnet (YAG) screen in order to position them at different longitudinal positions in the beam path, either in air or in a water phantom. The setup described was used both for dose-to-water calibrations for radiochromic films, and for beam profile measurement comparisons in air using both radiochromic films and the scintillating YAG screen.

3. Results

3.1. Photodetector evaluation measurements

With the single optical fibre and photodetectors assembled as shown in figure 2, measurements were taken for multiple consecutive pulses, specifically 100 pulses when using the SiPM or PMT as photodetector and 20 pulses for the CCD camera. The mean amplitude of the signal, recorded on a digitiser, was computed and the response of the optical fibre and photodetector at each pulse charge was obtained by integrating the mean signal in a time window of 400 ns. To check the linearity of the detector, the response was measured as a function of the charge per pulse. The increase of charge (and hence of the dose) per pulse was achieved by operating at the maximum stable bunch charge and then enlarge the pulse width by incrementing the number of bunches. The DPP values came from a corresponding charge to dose ratio obtained irradiating radiochromic film with the same pulse charges to which the optical fibre was exposed. A linear regression fit is then performed to describe the behaviour of the response of the fibre as function of DPP. The R^2 value, reduced chi-squared (also called mean squared weighted deviation $-\chi^2_\nu$) and p-value of the chi-squared value ($P(\chi^2)$) are computed and indicated in the relevant figure captions.

3.1.1. SiPM setup

The measurements using the SiPM as photodetector covered a range of pulse widths between 6.7 and 67 ns, corresponding to 10 bunches at 1.5 GHz, and to 200 bunches at 3 GHz spacing, respectively. The mean signal amplitude is shown in figure 5(a) and the response as a function of DPP in figure 5(b). The response of the optical fibre connected to the SiPM appears to be linear up to an equivalent dose per pulse of 38 Gy/pulse (65 ns pulse width with 3 GHz bunch spacing in order to reach upper DPP range) with a R^2 value of 0.994 for the fit. The response of the SiPM photodetector shows saturation above 50 bunches on the response traces shown in figure 5(a). Therefore the apparent linearity is likely to be from an increase in the area under the trace caused by the increase in pulse length and hence signal duration rather than from an increase in the signal amplitude. An error bar of $\pm 5\%$ was determined for the EBT3 and MDV3 DPP dose-to-water calibration which was obtained from the intrinsic uncertainty of the films, along with the pulse-by-pulse charge fluctuations and the standard deviation upon calculating the mean dose around the maximum of the Gaussian fit. Uncertainties in the fibre output were calculated from the standard deviation of the repeated measurements for each DPP, however these were negligible for each point for both the SiPM and PMT readout.

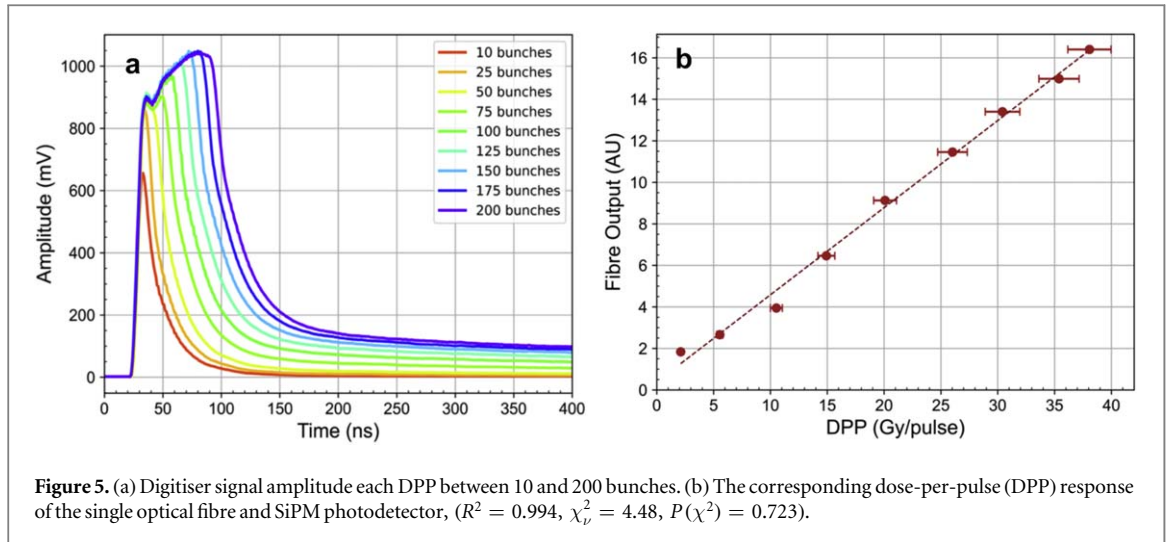


Figure 5. (a) Digitiser signal amplitude each DPP between 10 and 200 bunches. (b) The corresponding dose-per-pulse (DPP) response of the single optical fibre and SiPM photodetector, ($R^2 = 0.994$, $\chi^2_\nu = 4.48$, $P(\chi^2) = 0.723$).

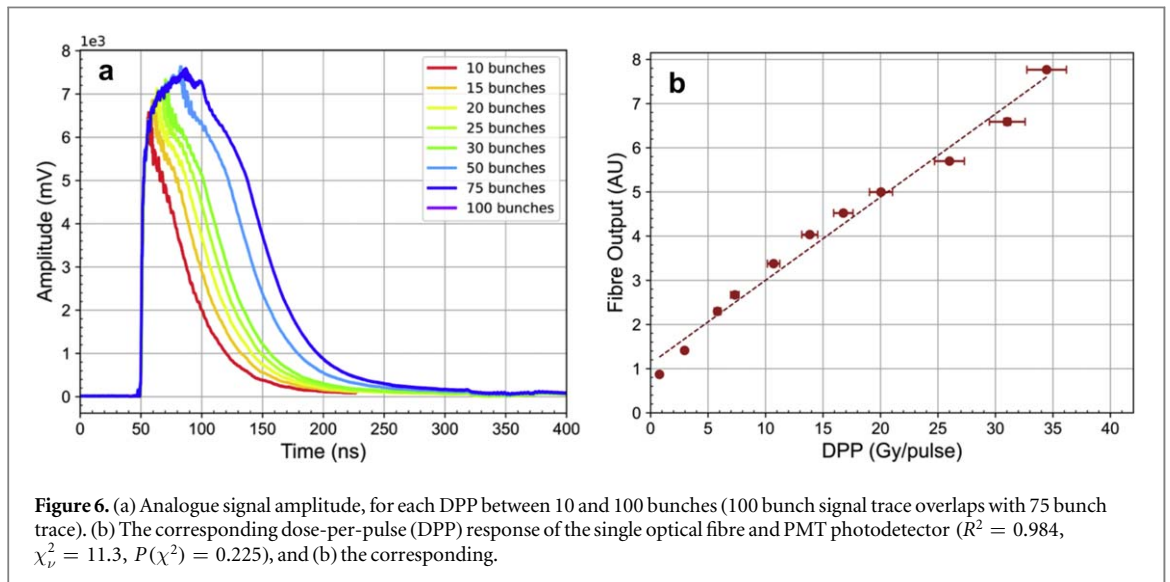


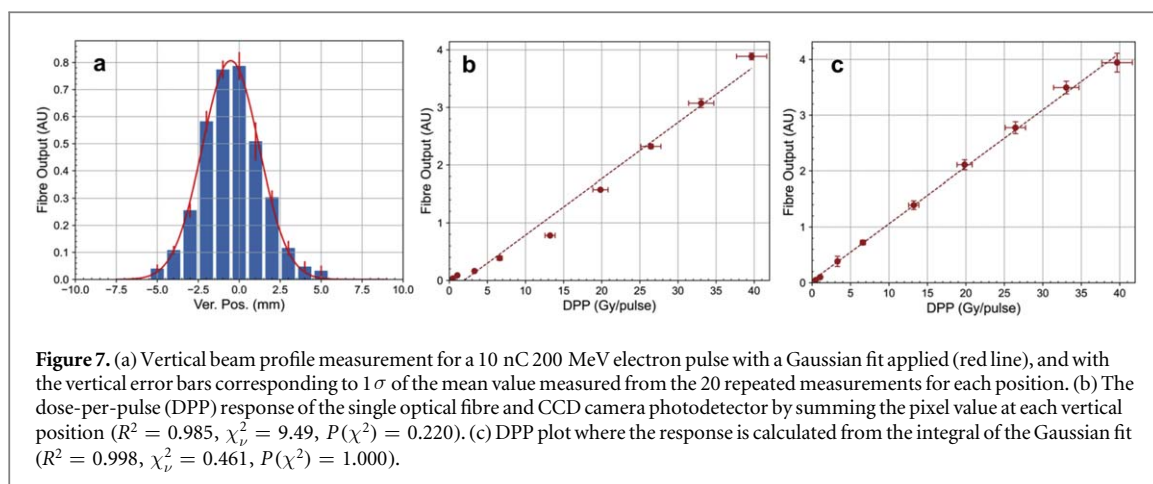
Figure 6. (a) Analogue signal amplitude, for each DPP between 10 and 100 bunches (100 bunch signal trace overlaps with 75 bunch trace). (b) The corresponding dose-per-pulse (DPP) response of the single optical fibre and PMT photodetector ($R^2 = 0.984$, $\chi^2_\nu = 11.3$, $P(\chi^2) = 0.225$), and (b) the corresponding.

3.1.2. PMT setup

The results obtained using the PMT as photodetector are shown in figures 6(a) and (b). In this case a range of pulse widths between 0.7 and 67 ns was used. Like the SiPM case, the signal amplitude saturates when the number of bunches is greater than 30, as it can be seen in figure 6(a). The response shown in figure 6(b) exhibits only approximate linearity up to a maximum achievable dose per pulse of 34 Gy/pulse with the linear fit having an R^2 value of 0.984. Several factors might contribute to the observed deviations from linearity. Saturation of the PMT is the likely cause of the onset of this deviation at about 10 Gy (30 bunches) and above. Subsequently, at longer pulse widths, the relation between the DPP and pulse width changes due to beam losses. This then decreases the instantaneous dose rate within the pulse and it appears as a larger integrated signal in figure 6(b), since the dose is delivered over a longer duration. In this case as well, like with the SiPM, the apparent linearity of the response to increasing DPP's will be from a greater integrated signal from the widening of the pulse duration.

3.1.3. CCD camera photodetector setup

The setup of the experiment was modified slightly when using the optical fibre and a CCD camera as photodetector, as can be seen in figure 2(b). A longer optical fibre (20 cm sensitive region, 1.2 m transport region) was used and the CCD camera was positioned in a light-tight 'black' box behind the beam dump. Since the photodetector was no longer in the beam contrary to the SiPM and PMT cases, there was space to mount the single fibre on a motorised stage with vertical movement and this made possible a measurement of the transverse profile of the beam. For each value of the beam charge (corresponding to a specific dose-per-pulse value) the optical fibre was moved vertically over the beam position at intervals of 1 mm between -5 and $+5$ mm with respect to the nominal centre ($y = 0$). For each pulse the mean value of the pixels over the area of the optical fibre



on the CCD camera image was taken. 20 measurements of consecutive pulses were acquired at each vertical position. The average of these 20 measurements (with an error assumed equal to the standard deviation) was taken as the response of the detector at the particular vertical position. This response as function of the vertical position of the fibre is shown in figure 7(a) for 10 nC pulse charge and 200 MeV electrons, as an example. This procedure allowed a reconstruction of the vertical profile of the beam. A Gaussian fit was then performed to the vertical profile of the beam for each value of the beam charge. To obtain the optical fibre response at a given DPP, two different methods were adopted and compared. The first consisted in summing the responses of the detector at each vertical position. The result is shown in figure 7(b) as a function of DPP. The other involved taking the integral of the Gaussian fit over the vertical profile for each dose per pulse and the results are shown in figure 7(c). Pulse widths in the range of 0.7–57 ns were used. The response of the detector can be seen to be linear up to a dose per pulse of 39 Gy/pulse, with an R^2 value of 0.985 and 0.998 for the summed response plot and the integral of the Gaussian plot, respectively. The response at DPP's of less than 5 Gy/pulse suffered from having a low signal-to-noise ratio (SNR). A better linear behaviour seems to be observed when using the integral of the Gaussian fit to the vertical profile for each DPP as detector response, however this method has larger error bars for each point due to uncertainties on the Gaussian fit therefore making it a less accurate method for determining the response of the fibre optic monitor. The differences between the two methods could be perhaps explained by the fact that the low intensity outer tails of the Gaussian beam are not efficiently detected due to the low SNR of the CCD camera. This under-response however, is compensated for when using the integral of the Gaussian fit.

From the standard deviation of the Gaussian fit to the vertical projection of the profile of the beam measured with the silica fibre and CCD camera for a pulse charge of 10 nC, (shown in figure 7(a)) the beam size was estimated to be 1.73 ± 0.09 mm. This can be compared to and is consistent with the value (1.83 ± 0.06 mm) measured on a YAG screen just behind the fibre installation.

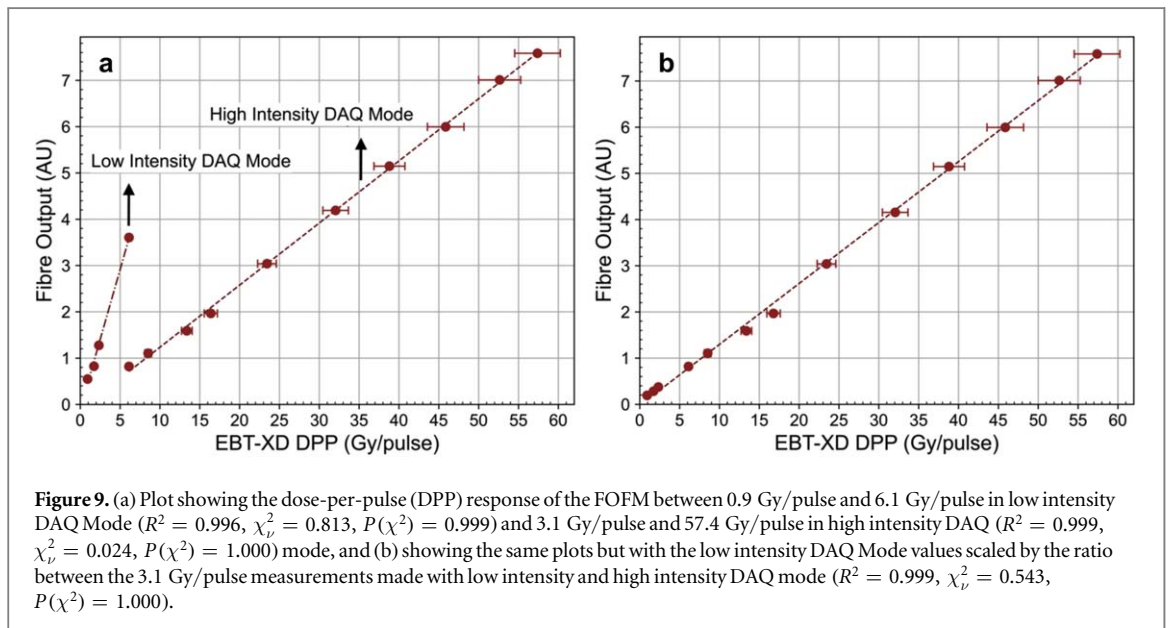
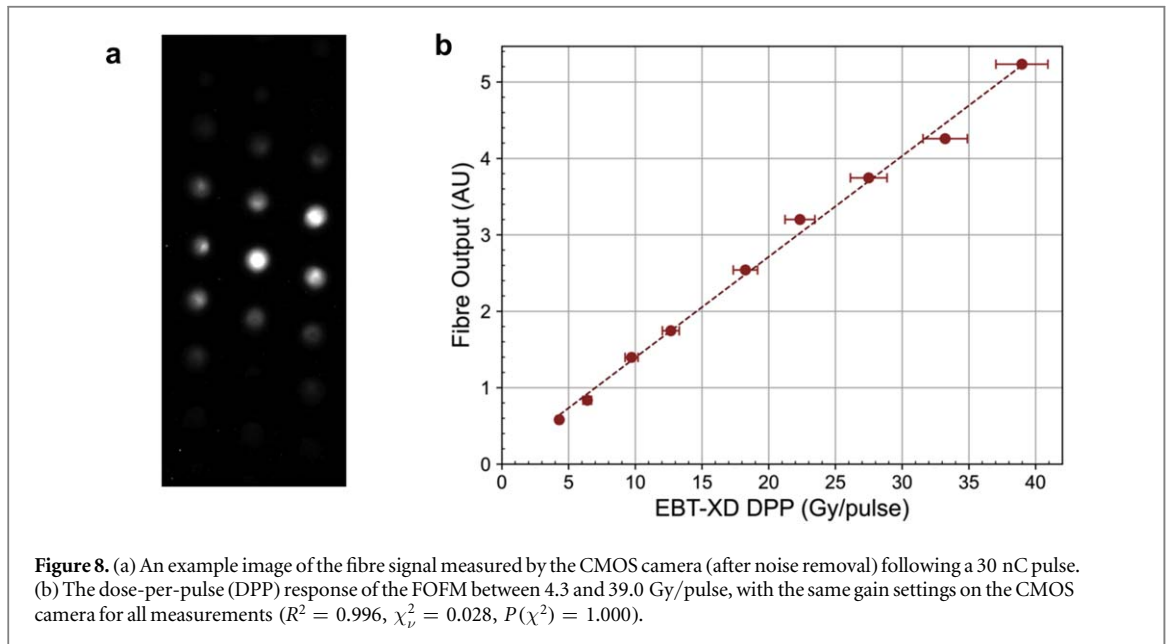
3.2. Optical fibre array measurements

To evaluate the performance of the FOFM optical fibre array for VHEE UHDR real-time beam monitoring using the setup shown in figure 3, a range of measurements were carried out with both 160 MeV and 200 MeV electrons. The investigation involved studies of the linearity of the response as function of the dose-per-pulse, using radiochromic films in water as reference as well as measurements of the beam profile, which was compared with that obtained using a scintillating YAG screen and radiochromic film.

3.2.1. Response linearity measurements

To evaluate the linearity of the response, at a given DPP, the sum of the pixel value from each individual fibre captured by the CMOS camera, such as that shown in figure 8(a), was measured. The results obtained with 200 MeV electrons and charge between 3.2 and 50.7 nC/pulse are shown in figure 8(b). Pulse widths in the range 9–105 ns were used, with a micropulse structure of 400 pC/bunch. For these measurements, the DPP varied from 4.3 to 39.0 Gy/pulse and the whole range was covered using the same CMOS camera settings, namely a normalised gain of 0.7. The data show that the FOFM exhibits a linear response over the entire range of DPP's, with the linear fit having an R^2 value of 0.996. Once more, an error bar of $\pm 5\%$ was determined for the EBT-XD DPP dose-to-water measurements. There was a variation of about $\pm 1\%$ between each shot for the same DPP, therefore error bars in the fibre output are not visible on the plots.

In order to extend the range of DPP's to values well below 5 Gy/pulse, two separate CMOS data acquisition (DAQ) settings were used for the low intensity and high intensity measurements. For the low intensity DAQ



Mode a normalised camera gain of 1 was used while, for high intensity DAQ Mode, this gain was set to 0.7, the same as shown in figure 8(b). The response of the FOFM when operated in these two modes is shown in figure 9(a) for 200 MeV electrons with 400 pC per bunch. In low intensity DAQ Mode, DPP's between 0.9 and 6.1 Gy/pulse were covered—with corresponding pulse widths of 0.7 to 9 ns—and showed a clear linear response with an R^2 value of 0.996. In high intensity DAQ Mode, DPP values between 6.1 and 57.4 Gy/pulse (pulse widths 9–130 ns) were used and again showed a linear response in the covered range, with an R^2 value of 0.999. To show the linearity of the FOFM response across the entire dynamic range, all measurements in which the two DAQ modes were used, the same DPP for the final measurement in low intensity DAQ Mode as the first measurement in high intensity DAQ Mode, and the low intensity DAQ Mode values were scaled accordingly. Figure 9(b) shows this, where the low intensity DAQ Mode data points from figure 9(a) have been scaled by the ratio of responses from the 6.1 Gy/pulse DPP in high intensity and low intensity DAQ modes. The response can still be seen to be linear across this entire range of DPP's, and has an R^2 value of 0.999. For the remainder of the DPP response linearity measurements, this scaling has been applied to all of the low intensity DAQ Mode data points.

The DPP response linearity was investigated for two different energies, the nominal energy at CLEAR of 200 MeV, and 160 MeV, to investigate the energy dependence of the response within the VHEE energy range. A comparison of the response of the optical fibre monitor to the two energies at DPP's between 0.9 and 38.8 Gy/

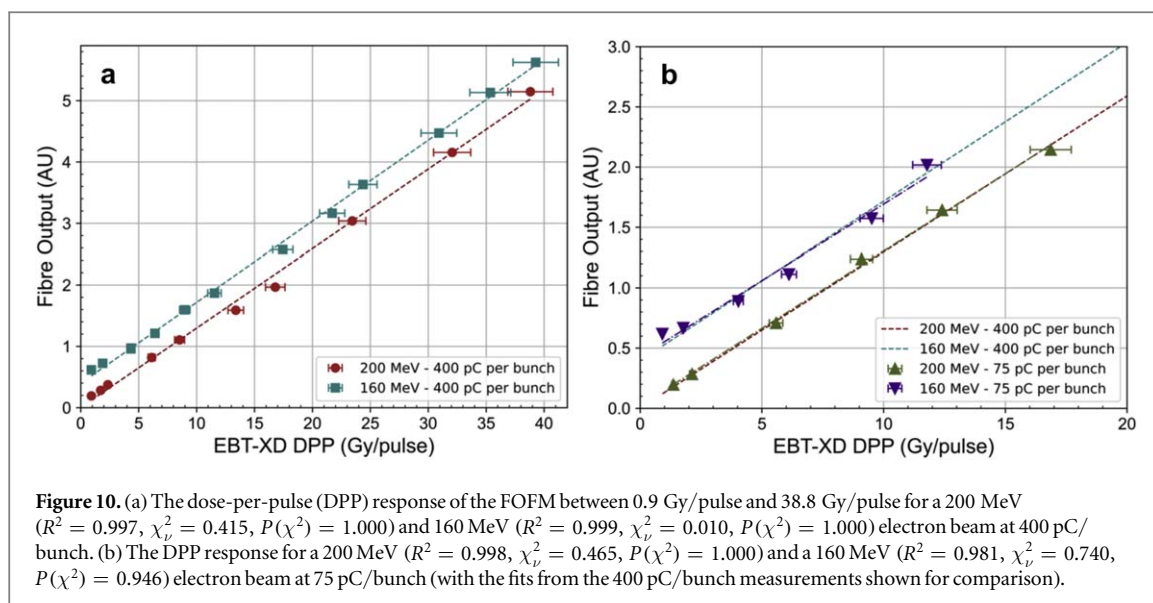


Table 1. The gradient values of the linear fit and their corresponding standard error for the measurements shown in figure 10.

Energy (MeV)	Charge per bunch (pC)	Gradient of linear fit	Standard error of gradient
200	400	0.130	0.002
200	75	0.128	0.002
160	400	0.132	0.001
160	75	0.127	0.007

pulse (with 400 pC/bunch and pulse widths of 0.7–76 ns) is shown in figure 10(a). The response for 200 MeV and 160 MeV can be seen to be linear, and of the similar gradient, the values for which are displayed in table 1. The R^2 value is 0.997 for the 200 MeV measurement and 0.999 for the 160 MeV measurement. In figure 10(a) constant offset between the 200 MeV and 160 MeV responses can be seen. This can be attributed to the difference in the percentage depth dose distribution for the two VHEE energies, and the constant position of the EBT-XD film, since the 160 MeV VHEE beam has an earlier fall-off, hence for the same pulse charge (and therefore the same fibre output), a smaller dose is deposited at the depth of the EBT-XD film (150 mm in water).

The instantaneous dose rate, i.e. the dose rate within each pulse of radiation, could potentially be a relevant parameter to elicit the FLASH effect. Therefore, it is important to establish that variations of this parameter do not affect the response of the beam monitor for the same DPP. For this purpose, the DPP response linearity measurements at 200 MeV and 160 MeV were repeated with two different pulse structures. It should be observed, however, that even with the same pulse width and charge, the dose rate within the pulse can vary. This variation is due to beam loading effects which are present for longer pulse widths and decrease the intensity of the later bunches on these longer trains. Since the charge per bunch is only measured for a single bunch per pulse, a range of instantaneous dose rates are given for each pulse structure. The first structure used was the same as for the results presented so far, i.e. the nominal and maximum charge per bunch of 400 pC, corresponding to an instantaneous dose rate range of $0.3 - 1 \times 10^9 \text{ Gy s}^{-1}$. The second bunch structure had a significantly lower charge per bunch, 75 pC, hence a longer pulse width for the same DPP, which corresponds to an instantaneous dose rate of $0.9 - 2.6 \times 10^8 \text{ Gy s}^{-1}$. The results obtained with this second bunch structure are shown in figure 10(b) for both 200 MeV and 160 MeV, with corresponding pulse widths of 5–130 ns. For comparison, the straight lines which are the results of the fit to the linear dependence of the response, obtained from the data with nominal charge per bunch shown in figure 10(a), are superimposed. The data displayed in figure 10(b), show that the linearity of the response with DPP is similar for both 200 MeV and 160 MeV energies, and for 400 pC/bunch and 75 pC/bunch pulse structures. The values for the gradients and the standard error of the gradient for these measurements are shown in table 1, where all gradients are in agreement within their respective standard errors.

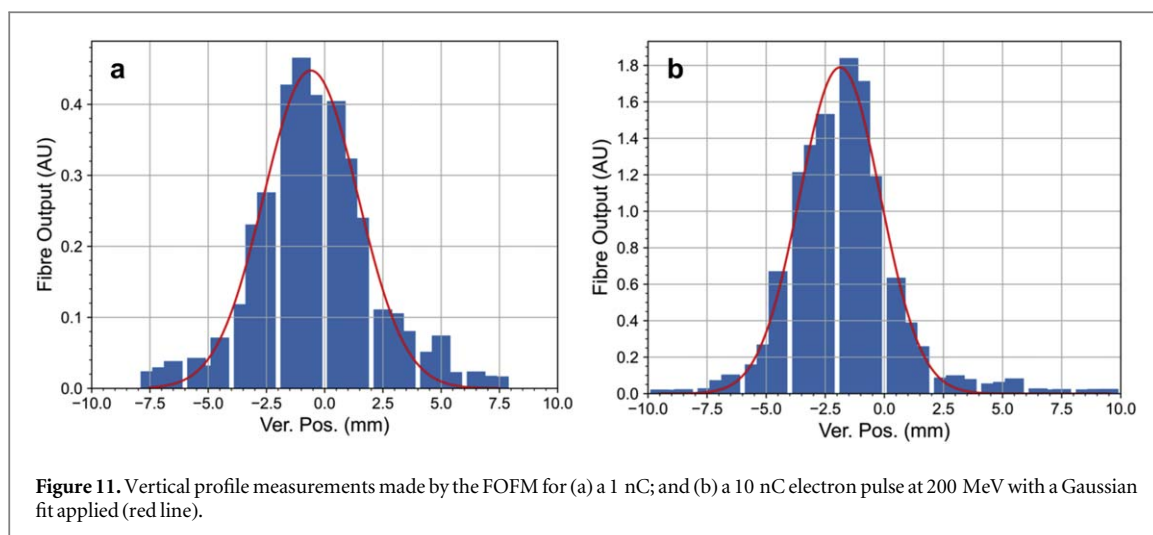


Figure 11. Vertical profile measurements made by the FOFM for (a) a 1 nC; and (b) a 10 nC electron pulse at 200 MeV with a Gaussian fit applied (red line).

Table 2. Vertical beam size measurements made with the FOFM, radiochromic film (with the type of film stated in square brackets), and scintillating YAG screen obtained from the standard deviation Gaussian fit applied to the vertical projection of the beam profile. The uncertainty of the beam size measurement is expressed as the error on the standard deviation of the 1D Gaussian fit.

Pulse charge (nC)	FOFM beam size (mm)	Film beam size (mm)	YAG beam size (mm)
1	2.02 ± 0.15	2.08 ± 0.03 [MD-V3]	1.98 ± 0.02
10	1.71 ± 0.09	1.66 ± 0.01 [HD-V2]	1.87 ± 0.01

3.2.2. Beam profile measurements

In order to reconstruct the profile of the beam measured by the FOFM, the pixel value of each of the individual fibres recorded by the CMOS camera was plotted against their corresponding vertical position. For the purpose of comparison and validation, in-air profile measurements were also made using radiochromic film (MD-V3 and HD-V2) and on a scintillating YAG screen—both positioned at 300 mm behind the FOFM. A Gaussian fit was applied to the vertical projection of the profile from both the radiochromic film and the scintillating YAG screen, and compared to the profile reconstructed from the FOFM.

Due to slight variations in the diameters and of the quality of the smoothness on the ends of the silica optical fibres, the relative response of each of the fibres varied slightly. To correct for this variation, the response of each of the individual optical fibres to the same beam intensity and position was recorded and then normalised to the mean response of all fibres in the FOFM. The nominal electron beam parameters at CLEAR were used for all of the beam profile measurements, namely 200 MeV energy and charge of 400 pC/bunch. Two different measurements were done on a single pulse, one at 1 nC/pulse, corresponding to 2.1 Gy/pulse, and another at 10 nC/pulse, corresponding to 17.0 Gy/pulse.

The vertical beam profile measured by the FOFM for a 1 nC pulse and a 10 nC pulse are shown in figures 11(a) and (b), respectively. The beam size, computed from the standard deviation of the Gaussian fit applied to the vertical profiles, was estimated to be 2.02 ± 0.15 mm for the 1 nC pulse and 1.71 ± 0.09 mm for the 10 nC pulse. The uncertainty is calculated from the error on the Gaussian fit. A comparison between these values and those obtained from the vertical profile projection from radiochromic films and a scintillating YAG screen is shown in table 2. Although with a larger uncertainty the results are consistent with those obtained using different techniques, with exception of the YAG screen for the 10 nC pulse.

4. Discussion

The purpose of the research presented in this paper is to show the development of a novel technology, based on the detection of Cherenkov light, alternative to transmission ionisation chambers for beam monitoring at UHDR for FLASH radiotherapy with VHEE, and eventually other modalities. The results presented demonstrate its ability to meet the requirements stated in the Introduction. The purpose of the measurements with a single optical fibre was to determine which of the photodetectors used exhibited the most suitable characteristics. Even though the SiPM and PMT showed a relatively linear response with increasing DPP ($R^2 = 0.994$ and 0.984 , respectively), the signal amplitude showed saturation and the apparent linearity could likely

be attributed to the widening of the pulse width. However, this demonstrates that these photodetectors have the advantage of a high time resolution that could be able to resolve the pulse width, even when operated under saturation conditions. Therefore the information could be used to monitor the instantaneous dose rate of the beam and a possible final prototype of the FOFM could incorporate a SiPM or a PMT attached to one of the fibres with the purpose of providing temporal information. A configuration similar to the one described in the paper by García Díez *et al* (2023) where the principle has been demonstrated using a plastic scintillator coupled to a SiPM via an optical fibre for monitoring the pulse structure in high dose rate proton therapy.

The CCD camera showed poor linearity ($R^2 = 0.985$) when summing the fibre response at each vertical position measurement, but conversely showed excellent linearity ($R^2 = 0.998$) when using the integral of the Gaussian fit applied to the profile for each DPP. This can likely be attributed to the Gaussian fit compensating for the under-response at intermediate DPP's due to the low SNR of the CCD camera, meaning the low intensity tails of the beam are not accurately measured. Furthermore, the relatively low SNR of the CCD camera meant that the optical fibre had to be positioned at an angle in order for a large enough Cherenkov signal to reach the CCD.

The fused silica optical fibres were chosen for the FOFM since the lack of coating and cladding (which had a similar refractive index to the silica core) permitted a larger transmission of the Cherenkov signal to the end of the optical fibres. The CMOS camera was chosen in this case instead of a CCD camera since it has all the advantageous properties of the latter with the addition of a larger dynamic range and a faster frame rate. Since the maximum p.r.f at CLEAR is 10 Hz, a CMOS camera with a frame rate of 42 frame s^{-1} was perfectly adequate for the measurements performed, a larger frame rate being not necessary at the CLEAR repetition frequency. However, proposed clinical VHEE linacs are likely to have a p.r.f of at least 100 Hz in order to deliver the prescribed dose over multiple pulses within FLASH timescales. There are commercially available cameras from the same manufacturer with the same properties and resolution but with a frame rate of 168 frame s^{-1} , or at frame rates >500 frame s^{-1} with a reduced resolution. A CMOS camera has the additional advantage over SiPM and PMT of being able to image multiple optical fibres simultaneously (in the case discussed in this paper the entire array of 28 fibres), compared to requiring one photodetector per optical fibre sensor.

Arguably the most important requirement for a UHDR beam monitor is the detector's capability to respond linearly to dose and dose rate. The response of the currently used transmission ionisation monitor chambers has been shown to deviate from linearity at dose rates of <0.1 Gy/pulse with 10 MeV electrons (Konradsson *et al* 2020). In this work it has been demonstrated that the FOFM response is linear with dose and dose rate between 4.3 Gy/pulse and 39.0 Gy/pulse, when operated with the same DAQ settings (figure 8), and between 0.9 and 57.4 Gy/pulse (equivalent to range of 9.0–574 Gy s^{-1} mean dose rate at the maximum CLEAR p.r.f. of 10 Hz), when operated with two different DAQ settings for low DPP and high DPP (figures 9(a) and (b)).

Other novel UHDR beam monitors are under development. ICTs have been shown to have a linear response beyond 15 Gy/pulse with 6 MeV electrons and require two separate modes for CONV and UHDR dose rates (Oesterle *et al* 2021); linearity of the response was shown up to 20 Gy/pulse with 7 MeV electrons (Triglio *et al* 2022) for the FLASHDC air fluorescence monitor, and up to 2 Gy/pulse (mean dose rate of 30 Gy s^{-1}) with 9 MeV electrons (Romano *et al* 2023) for SiC detectors. The FBSM reportedly showed dose rate linearity in their response up to 234 Gy s^{-1} with 8 MeV electrons (Levin *et al* 2023). In the two FLASH radiotherapy patient trials to date, conducted using 5.6 MeV electrons (Bourhis *et al* 2019) and 200 MeV protons (Mascia *et al* 2023), radiation was delivered using single fraction in both cases, with a total prescribed dose of 15 Gy delivered at 166.7 Gy s^{-1} (1.5 Gy/pulse) and 8 Gy with a quasi-continuous dose rate of 60 Gy s^{-1} for the electrons and protons, respectively. Furthermore, significant work has also been published on the treatment plans proposed for VHEE, suggesting minimum beam intensities of 9.375×10^{11} electrons s^{-1} for $>90\%$ of the PTV, to receive a dose-averaged dose rate in excess of 40 Gy s^{-1} (Zhang *et al* 2023). Assuming similar beam parameters and size at which the FOFM was tested with at the CLEAR facility, the above intensity requirement translates into a minimum DPP of ~ 23 Gy/pulse at 10 Hz p.r.f, or ~ 2.3 Gy/pulse at 100 Hz p.r.f. Therefore, the measurements described in this paper demonstrate that indeed the FOFM exhibits the response linearity required for dose monitoring for VHEE into—and possibly beyond—the UHDR regime necessary for inducing the FLASH effect.

It is likely that the clinical translation of VHEE radiotherapy will make use of electron beams of different energies, to provide conformal dose distributions to tumours of different depths. It is therefore important that any adopted beam monitoring technology does not exhibit an energy dependence. The validity of this premise was tested as part of the experiments for validating the FOFM with 200 MeV and 160 MeV electron energies. The results, presented in figure 10 and table 1, show that the gradients of the slope of the straight line fits describing the DPP response at the two different energies are within close agreement, demonstrating therefore a consistent response within this energy range.

Furthermore, differing instantaneous dose rates will likely be used both in pre-clinical and clinical experiments, so it is therefore necessary that the response of the beam monitor is independent of this. The results of this comparison for the FOFM can also be seen in figure 10 and table 1, whereby the gradients of the two

separate instantaneous dose rates for 200 MeV and 160 MeV are also all within close agreement. Since the values for the gradient for the 75 pC/bunch measurements at both energies are within their respective standard error of the gradients for the 400 pC/bunch at both energies, the response can be considered to be independent of the instantaneous dose rate. The slight difference and larger standard error visible in table 1 between the two instantaneous dose rates at 160 MeV can likely be attributed to the associated changes of beam parameters that come with altering the charge per bunch for energy that is not nominal for CLEAR operation.

Most of the currently employed conventional radiotherapy monitor chambers do not provide beam profile measurements, but instead they monitor the flatness and symmetry of the beam, to ensure it stays within pre-defined tolerances. However, given the added uncertainties and risks that are associated with delivering the prescribed dose at UHDR, pulse-by-pulse measurements of the beam profile would be an additional level of quality assurance for dose delivery during FLASH radiotherapy. Furthermore, if PBS were to be used for the delivery of VHEE beams (either at conventional or ultrahigh dose rates), the FOFM could provide pulse-by-pulse beam position measurements in addition to profile measurements. The results of the beam profile measurements for one single 1 nC and 10 nC electron pulse, shown in figures 11(a) and (b), were found to be in reasonable agreement with measurements on radiochromic film and YAG screen. For the 1 nC pulse both the measurement comparisons from the MDV3 film and YAG screen were within the errors of the FOFM beam size measurements. For the 10 nC pulse the beam profile measurement with the HDV2 film was still within the uncertainty range of the FOFM measurement. Whereas the comparison between the FOFM and YAG screen measurement showed a larger difference and was outside of the FOFM uncertainty range. This larger beam size observed at high charges in the YAG scintillating screen for in-air measurements has also been reported previously at CLEAR and further studies are underway to understand and characterise this effect (Rieker *et al* 2023). The beam profile measurements made FBSM for UHDR beam monitoring were reported to have fits that agree with those on Gafchromic EBT-XD films within 1.4% (Levin *et al* 2023). One of the limiting factors that cause the larger discrepancies seen with the FOFM profile measurements; the first being the spatial resolution being limited to the diameter and spacing of the optical fibres, which in this case is 0.5–1 mm. In spite of the limitation, the measurements show that the FOFM is capable of providing pulse-by-pulse measurements of the beam profile with good accuracy. The final design of the FOFM will incorporate two optical fibre arrays to provide beam profile measurements in both the x and y -axis.

The work presented in this paper served the purpose of proof-of-principle measurements, demonstrating that the FOFM is capable of providing real-time pulse-by-pulse beam profile measurements and give a linear response with dose deposited at a reference depth in water into the UHDR regime. In order to ensure that such a monitor would be feasible for use on a clinical VHEE machine, further measurements are necessary, however. The long-term stability of the monitor response (particularly for dose prediction and monitoring) will have to be verified, along with the characterisation of any ageing or deteriorations of the response of the fibres following irradiations with doses in the range of that expected throughout the lifetime of a typical monitor chamber. Radiation hardness tests of the silica fibres used in the experiment described in this paper are currently being carried out at the IRRAD facility at CERN, with 24 GeV protons up to doses on the order of MGy's and both the Cherenkov signal from the beam and light transmission from a bulb are being measured (Buchanan *et al* 2023). Similar tests will be carried out at the CLEAR facility investigating the stability of the response and of its linearity, following irradiations of large doses (up to hundreds of kGy).

5. Conclusions

To facilitate pre-clinical experiments and the eventual clinical translation of FLASH radiotherapy with VHEE, a new technological solution for real-time beam monitoring is required, given that saturation effects are present at UHDR in transmission ionisation monitor chambers currently in use. In this paper, a device in which the Cherenkov light produced by high energy electrons traversing silica optical fibres—single or arranged in an array (FOFM)—is detected by different photodetectors, is proposed as a possible solution. While recently published results on a similar area of research have shown advances on the development of beam monitoring technologies for UHDR using devices such as ICTs, SiC detectors and scintillating screens, the results on the FOFM presented in this article are the first in which such a technology is considered for UHDR online beam monitoring for VHEE beams. The initial results, obtained with 200 MeV and 160 MeV electron beams at the CLEAR facility at CERN, showed that the FOFM beam monitor with a CMOS Camera as photodetector exhibited a linear response with DPP from 0.9 to 57.4 Gy/pulse, i.e. over the entire range it was tested. It was also demonstrated that the response did not depend on energy and instantaneous dose rate, both important factors for monitoring the delivery of the VHEE dose at UHDR. Furthermore, the FOFM was able to perform accurate pulse-by-pulse measurements of the beam profile, showing agreement with the same profile measurements performed using radiochromic film.

In addition, the use of either a SiPM or a PMT connected to a single fibre as part of the optical fibre array in the FOFM would be able to provide information about the instantaneous dose rate of the beam, even when operated under saturation conditions, due to the good time resolution of these photodetectors. Consequently, the work presented has shown that a fibre optic beam monitor, such as the one proposed in this paper, is a promising candidate for real-time beam profile and dose monitoring for FLASH radiotherapy with VHEE.

One current limitation of the study is using radiochromic films calibrated to 5.5 MeV electrons to provide dose-to-water characterisations for the fibre optic monitor. Whilst some studies point to there being little-to-no energy dependence across a large range of electron energies, such films do exhibit energy-dependence for other modalities and therefore further studies would benefit from using a radiochromic film calibration with VHEE beams once the procedure is available. Subsequently, using other detectors and passive dosimeters to provide such characterisations would add further reliability to the measurements.

Further work is currently ongoing to fully characterise the single optical fibre array and develop a full scale prototype of the FOFM, consisting of two separate arrays to provide profile measurements in both transverse dimensions of the beam. The full prototype will need to be tested with other radiation modalities at UHDR as well as being further characterised with VHEE beams at the CLEAR facility. The additional profile measurements should also be made with magnified uniform beams in addition to the VHEE Gaussian pencil beams used at the CLEAR facility. These studies will involve further measurements on the linearity of the response as well as beam profile comparisons, radiation hardness, stability of the response, and dose prediction.

Acknowledgments


This research was funded by an STFC 2020 Grant No. 2432490. This project has also received funding from the European Union's Horizon Europe Research and Innovation programme under Grant Agreement No. 101057511 (EURO-LABS).

Data availability statement

All data that support the findings of this study are included within the article (and any supplementary information files).

ORCID iDs

Joseph J Bateman  <https://orcid.org/0000-0002-5967-6748>

Robert Garbrecht Larsen  <https://orcid.org/0009-0001-2605-4643>

Manjit Dosanjh  <https://orcid.org/0000-0003-1378-349X>

References

- Allegrini O *et al* 2021 Characterization of a beam-tagging hodoscope for hadrontherapy monitoring *J. Instrum.* **16**
- Ashraf M R, Rahman M, Cao X, Duval K, Williams B B, Jack Hoopes P, Gladstone D J, Pogue B W, Zhang R and Bruza P 2022 Individual pulse monitoring and dose control system for pre-clinical implementation of FLASH-RT *Phys. Med. Biol.* **67**
- Ashraf M R, Rahman M, Zhang R, Williams B B, Gladstone D J, Pogue B W and Bruza P 2020 Dosimetry for FLASH radiotherapy: a review of tools and the role of radioluminescence and cherenkov emission *Front. Phys.* **8** 2296–424X
- Bazalova-Carter M, Qu B, Palma B, Hårdemark B, Hynning E, Jensen C, Maxim P G and Loo B W 2015 Treatment planning for radiotherapy with very high-energy electron beams and comparison of VHEE and VMAT plans *Med. Phys.* **42**
- Böhlen T T, Germond J F, Traneus E, Bourhis J, Vozenin M C, Bailat C, Bochud F and Moeckli R 2021 Characteristics of very high-energy electron beams for the irradiation of deep-seated targets *Med. Phys.* **48**
- Bourhis J *et al* 2019 Treatment of a first patient with FLASH-radiotherapy *Radiother. Oncol.* **139**
- Buchanan E *et al* 2023 Radiation hard beam profile monitors for the north experimental beamlines CERN *Proc. 12th Int. Beam Instrum. Conf. (IBIC'23)* pp 321–5
- Chan M F, Park J, Aydin R and Lim S B 2023 Technical note: energy dependence of the gafchromic EBT4 film: dose-response curves for 70 kV, 6 MV, 6 MV FFF, 10 MV FFF, and 15 MV x-ray beams *Med. Phys.* **50**
- DesRosiers C, Moskvina V, Bielajew A F and Papiez L 2000 150–250 MeV electron beams in radiation therapy *Phys. Med. Biol.* **45**
- Faillace L *et al* 2022 Perspectives in linear accelerator for FLASH VHEE: study of a compact C-band system *Physica Med.* **104**
- Favaudon V *et al* 2014 Ultrahigh dose-rate FLASH irradiation increases the differential response between normal and tumor tissue in mice *Sci. Transl. Med.* **6** p245–93
- Favaudon V, Lentz J M, Heinrich S, Patriarca A, de Marzi L, Fouillade C and Dutreix M 2019 Time-resolved dosimetry of pulsed electron beams in very high dose-rate, FLASH irradiation for radiotherapy preclinical studies *Nucl. Instrum. Methods Phys. Res. A* **944**
- García Díez M, Espinosa Rodríguez A, Sánchez Tembleque V, Sánchez Parcerisa D, Valladolid Onecha V, Vera Sanchez J A, Mazal A, Fraile L M and Udias J M 2023 Technical note: measurement of the bunch structure of a clinical proton beam using a SiPM coupled to a plastic scintillator with an optical fiber *Med. Phys.* **50**

- Guan F, Chen H, Draeger E, Li Y, Aydin R, Tien C J and Chen Z 2023a Characterization of Gafchromic™ EBT4 film with clinical kV/MV photons and MeV electrons *Precis. Radiat. Oncol.* **7**
- Guan F et al 2023b Dosimetric response of Gafchromic™ EBT-XD film to therapeutic protons *Precis. Radiat. Oncol.* **7**
- Hart A, Cecchi D, Giguère C, Larose F, Therriault-Proulx F, Esplen L, Beaulieu L and Bazalova-Carter M 2022 Lead-doped scintillator dosimeters for detection of ultrahigh dose-rate x-rays *Phys. Med. Biol.* **67**
- Jaccard M, Petersson K, Buchillier T, Germond J F, Durán M T, Vozenin M C, Bourhis J, Bochud F O and Bailat C 2017 High dose-per-pulse electron beam dosimetry: usability and dose-rate independence of EBT3 gafchromic films: usability *Med. Phys.* **44**
- Jaccard M, Durán M T, Petersson K, Germond J F, Liger P, Vozenin M C, Bourhis J, Bochud F and Bailat C 2018 High dose-per-pulse electron beam dosimetry: commissioning of the oriatron eRT6 prototype linear accelerator for preclinical use: commissioning *Med. Phys.* **45**
- Jeong D H, Lee M, Lim H, Kang S K, Lee K, Lee S J, Kim H, Han W K, Kang T W and Jang K W 2021 Optical filter-embedded fiber-optic radiation sensor for ultra-high dose rate electron beam dosimetry *Sensors* **21**
- Jolly S, Owen H, Schippers M and Welsch C 2020 Technical challenges for FLASH proton therapy *Phys. Med.* **78**
- Kanouta E, Poulsen P R, Kertzsch G, Sitarz M K, Sørensen B S and Johansen J G 2023 Time-resolved dose rate measurements in pencil beam scanning proton FLASH therapy with a fiber-coupled scintillator detector system *Med. Phys.* **50**
- Kokurewicz K et al 2019 Focused very high-energy electron beams as a novel radiotherapy modality for producing high-dose volumetric elements *Sci. Rep.* **9** 10837
- Kokurewicz K et al 2021 An experimental study of focused very high energy electron beams for radiotherapy *Commun. Phys.* **4** 3
- Konradsson E, Ceberg C, Lempart M, Blad B, Bäck S, Knöös T and Petersson K 2020 Correction for ion recombination in a built-in monitor chamber of a clinical linear accelerator at ultra-high dose rates *Radiat. Res.* **194** 580–6
- Korysko P et al 2023a VHEE and ultra high dose rate radiotherapy studies in the CLEAR user facility *Proc. IPAC'23* pp 5063–6
- Korysko P et al 2023b The CLEAR user facility: a review of the experimental methods and future plans *Proc. IPAC'23* pp 876–9
- Lagzda A, Angal-Kalinin D, Jones J, Aitkenhead A, Kirkby K J, MacKay R, van Herk M, Farabolini W, Zeeshan S and Jones R M 2020 Influence of heterogeneous media on very high energy electron (VHEE) dose penetration and a Monte Carlo-based comparison with existing radiotherapy modalities *Nucl. Instrum. Methods Phys. Res.* **482**
- Leverington B D, Dziewiecki M, Renner L and Runze R 2018 A prototype scintillating fibre beam profile monitor for Ion Therapy beams *J. Instrum.* **13**
- Levin D S et al 2023 A scintillator beam monitor for real-time FLASH radiotherapy arXiv:2305.15306v1
- Loo B W, Schuler E, Lartey F M, Rafat M, King G J, Trovati S, Koong A C and Maxim P G 2017 (P003) Delivery of ultra-rapid flash radiation therapy and demonstration of normal tissue sparing after abdominal irradiation of mice *Int. J. Radiat. Oncol. Biol. Phys.* **98**
- Mascia A E et al 2023 Proton FLASH radiotherapy for the treatment of symptomatic bone metastases: the FAST-01 nonrandomized trial *JAMA Oncol.* **9**
- McManus M, Romano F, Lee N D, Farabolini W, Gilardi A, Royle G, Palmans H and Subiel A 2020 The challenge of ionisation chamber dosimetry in ultra-short pulsed high dose-rate very high energy electron beams *Sci. Rep.* **10** 9089
- Micke A, Lewis D F and Yu X 2011 Multichannel film dosimetry with nonuniformity correction *Med. Phys.* **38** 2523–34
- Montay-Gruel P et al 2017 Irradiation in a flash: unique sparing of memory in mice after whole brain irradiation with dose rates above 100 Gy s⁻¹ *Radiother. Oncol.* **124**
- Montay-Gruel P et al 2019 Long-term neurocognitive benefits of FLASH radiotherapy driven by reduced reactive oxygen species *PNAS* **166**
- Montay-Gruel P et al 2021 Hypofractionated FLASH-RT as an effective treatment against glioblastoma that reduces neurocognitive side effects in mice *Clin. Cancer Res.* **27**
- Montay-Gruel P, Corde S, Laissue J A and Bazalova-Carter M 2022 FLASH radiotherapy with photon beams *Med. Phys.* **49**
- Muscato A et al 2023 Treatment planning of intracranial lesions with VHEE: comparing conventional and FLASH irradiation potential with state-of-the-art photon and proton radiotherapy *Front. Phys.* **11** 2296–424X
- Oesterle R, Gonçalves Jorge P, Grilj V, Bourhis J, Vozenin M C, Germond J F, Bochud F, Bailat C and Moeckli R 2021 Implementation and validation of a beam-current transformer on a medical pulsed electron beam LINAC for FLASH-RT beam monitoring *J. Appl. Clin. Med. Phys.* **22**
- Ortega Ruiz I, Fosse L, Franchi J, Frassier A, Fullerton J, Kral J, Lauener J, Schneider T and Tranquille G 2020 The XBPF, a new multipurpose scintillating fibre monitor for the measurement of secondary beams at CERN *Nucl. Instrum. Methods Phys. Res. A* **951**
- Petersson K, Jaccard M, Germond J F, Buchillier T, Bochud F, Bourhis J, Vozenin M C and Bailat C 2017 High dose-per-pulse electron beam dosimetry—a model to correct for the ion recombination in the advanced markus ionization chamber *Med. Phys.* **44**
- Poppinga D, Kranzer R, Farabolini W, Gilardi A, Corsini R, Wyrwoll V, Looe H K, Delfs B, Gabrisch L and Poppe B 2020 VHEE beam dosimetry at CERN linear electron accelerator for research under ultra-high dose rate conditions *Biomed. Phys. Eng. Express* **7**
- Rieker V et al 2023 Beam instrumentation for real time FLASH dosimetry: experimental studies in the CLEAR facility *Proc. IPAC'23* pp 5032–5
- Romano F et al 2023 First characterization of novel silicon carbide detectors with ultra-high dose rate electron beams for FLASH radiotherapy *Appl. Sci.* **13**
- Romano F, Bailat C, Jorge P G, Lerch M L F and Darafsheh A 2022 Ultra-high dose rate dosimetry: challenges and opportunities for FLASH radiation therapy *Med. Phys.* **49**
- Rothwell B C, Kirkby N F, Merchant M J, Chadwick A L, Lowe M, Mackay R I, Hendry J H and Kirkby K J 2021 Determining the parameter space for effective oxygen depletion for FLASH radiation therapy *Phys. Med. Biol.* **66**
- Schuler E, Eriksson K, Hynning E, Hancock S L, Hiniker S M, Bazalova-Carter M, Wong T, Le Q T, Loo B W and Maxim P G 2017 Very high-energy electron (VHEE) beams in radiation therapy; treatment plan comparison between VHEE, VMAT, and PPBS *Med. Phys.* **44**
- Sjobak K N et al 2019 Status of the CLEAR electron beam user facility at CERN *Int. Particle Accelerator Conf.*
- Subiel A et al 2014 Dosimetry of very high energy electrons (VHEE) for radiotherapy applications: using radiochromic film measurements and Monte Carlo simulations *Phys. Med. Biol.* **59**
- Trigilio A et al 2022 The FlashDC project: development of a beam monitor for FLASH radiotherapy *Nucl. Instrum. Methods Phys. Res. A* **1041**
- Vanreusel V et al 2022 Point scintillator dosimetry in ultra-high dose rate electron 'FLASH' radiation therapy: a first characterization. *Phys. Med.* **103**
- Villoing D et al 2022 Technical note: proton beam dosimetry at ultra-high dose rates (FLASH): evaluation of GAFchromic™ (EBT3, EBT-XD) and OrthoChromic (OC-1) film performances *Med. Phys.* **49**
- Vozenin M C, Bourhis J and Durante M 2022 Towards clinical translation of FLASH radiotherapy *Nat. Rev. Clin. Oncol.* **19**
- Vozenin M C, Hendry J H and Limoli C L 2019 Biological benefits of ultra-high dose rate FLASH radiotherapy: sleeping beauty awoken *Clin. Oncol.* **31**

- Whitmore L, Mackay R I, van Herk M, Jones J K and Jones R M 2021 Focused VHEE (very high energy electron) beams and dose delivery for radiotherapy applications *Sci. Rep.* **11** 14013
- Wilson J D, Hammond E M, Higgins G S and Petersson K 2020 Ultra-high dose rate (FLASH) radiotherapy: silver bullet or fool's gold? *Frontiers Oncol.* **9** 1563
- Zha H and Grudiev A 2017 Design of the compact linear collider main linac accelerating structure made from two halves *Phys. Rev. Accel. Beams* **20** 042001
- Zhang G, Zhang Z, Gao W and Quan H 2023 Treatment planning consideration for very high-energy electron FLASH radiotherapy *Phys. Med.* **107**